Stable Crosslinked Vinyl-Addition-Type Polynorbornene Graft Copolymer Proton-Exchange Membranes

Shufang Liu, Yiwang Chen, Xiaohui He, Lie Chen, Weihua Zhou

Institute of Polymers/Institute for Advanced Study, Nanchang University, 999 Xuefu Avenue, Nanchang 330031, China

Received 6 September 2010; accepted 17 October 2010
DOI 10.1002/app.33638
Published online 28 February 2011 in Wiley Online Library (wileyonlinelibrary.com).

ABSTRACT: The graft copolymer poly(butoxymethylene norbornene-*co*-norbornenemethylene bromoisobutyrylate) [P(BN/NB)]-*graft*-poly(hydroxyethyl methacrylate) (PHEMA) was synthesized by the atom transfer radical polymerization of 2-hydroxyethyl methacrylate from a copolymer prepared by two functional norbornene monomers via a vinyl addition mechanism. The graft copolymer P(BN/NB)-*g*-PHEMA was further crosslinked with 4,5-imidazole dicarboxylic acid (IDA) and then doped with phosphoric acid (H_3PO_4) to form imidazole–H_3PO_4 complexes. The results show that the polynorbornene backbone and crosslinked micromorphology produced low methanol permeability in the membranes (from 1.5×10^{-7} to 3.8×10^{-6} cm^2/s) and endowed the membranes with good mechanical properties (with elastic modulus values of 692.7 to 159.7 MPa, elongation at break values from 2.7 to 22.7%, and tensile strength at break values from 14.4 to 5.5 MPa) and excellent thermal stability (up to 280°C). Furthermore, the proton conductivities of the membranes increased with increasing temperature and increasing content of IDA/H_3PO_4 in the membranes. © 2011 Wiley Periodicals, Inc. J Appl Polym Sci 121: 1166–1175, 2011

Key words: addition polymerization; atom transfer radical polymerization (ATRP); high performance polymers

INTRODUCTION

Polymer electrolyte membrane fuel cells (PEMFC) are potentially one of the best candidates for the replacement of conventional internal combustion engines in automobiles, stationary power, and batteries in portable electronic devices because of their high energy efficiency and environmental friendliness.[1] Among various PEMFCs, direct methanol fuel cells (DMFCs) are suited for portable devices or transportation applications because of their high energy density at low operating temperatures and their ease in handling liquid fuel.[2,3] One of the most crucial elements of DMFCs is the polymer electrolyte membrane (PEM) layer, across which protons are transported. Criteria for practical PEMs are chemical stability, good electrode adhesion properties, high proton conductivity, and low methanol permeability.[4]

PEMFCs commonly use Nafion perfluorinated sulfonic acid membrane as the representative because Nation series exhibit excellent thermal, mechanical, and electrochemical properties along with a reasonable cell performance.[5] However, the Nafion series also has some significant drawbacks, including a high cost and considerable methanol crossover when it is used in DMFCs; these result in a decreased efficiency. Thus, many materials, including modified sulfonated Nafion, sulfonated polyimide, sulfonated poly(ether ketone)s, sulfonated poly(arlyene ether sulfone), and sulfonated polybenzimidazole, have been developed for this purpose and have shown some degree of success,.[6–9] For the sulfonated polymer membrane, the higher the sulfonation degree is, the higher the proton conductivity is, but with the high sulfonation degree, the membrane ion exchange capacity is too high; this increases the water uptake and methanol permeability and reduces the performance of DMFCs. Hence, there is a need to develop a membrane material that can deliver a high proton conductivity combined with a low methanol permeability.

The morphology of the membrane is very important for proton conductivity, and a microphase-separated morphology may favor the easiest transport of protons in the membranes.[10] The methanol

Correspondence to: Y. Chen (ywchen@ncu.edu.cn), L. Chen (chenlienc@163.com), and X. He (hexiaohuishulei@yahoo.com.cn).

Contract grant sponsor: Program for International Cooperation in Jiangxi Provincial Department of Science and Technology; contract grant number: 2009BHC00200.

Contract grant sponsor: Program for Innovative Research Team in University of Jiangxi Province.

© 2011 Wiley Periodicals, Inc.

permeability is often attributed to the membrane microstructures;[11,12] one promising approach is to introduce new designs that differ from the existing ones at a fundamental molecular chemistry level,[13,14] and crosslinking is becoming an effective way of improving the overall performance of the film in the preparation of proton-exchange membranes.[15–24]

Polynorbornene materials continue to be of interest for gas transport and ionic transport applications because of their high thermal stability, good mechanical properties, and excellent resistance to plasma etching. Several sulfonated polynorbornene derivatives with high proton conductivities used as PEMs have been synthesized by ring-opening methathesis polymerization, followed by the treatment of sulfonating agents of acetyl sulfate or hydrogeneration of the main chains.[25–27] Compared to ring-opening methathesis polymerization of norbornene, the vinyl addition polymerization of norbornene yields a polynorbornene with better properties and higher performance. In particular, the low methanol permeability of the vinyl-addition-type polynorbornene has also evoked people's interest in its application in DMFCs. However, vinyl-type polynorbornene has rarely been reported in the PEM field to this point.

With the aim of reducing methanol crossover, obtaining a good proton conductivity, and improving the mechanical properties, in this study, we examined on a novel crosslinked functional polynorbornene graft copolymer proton conducting membrane: poly(butoxymethylene norbornene-*co*-norbornenemethylene bromoisobutyrylate) [P(BN/NB)]-*g*-poly(hydroxyethyl methacrylate) (PHEMA)/4,5-imidazole dicarboxylic acid (IDA)/phosphoric acid (H_3PO_4). The approach was based on the polymerization of the functional norbornene by a vinyl addition mechanism with bis(β-ketonaphthylamine) nickel(II) as a catalyst. We then grafted the product with PHEMA via atom transfer radical polymerization (ATRP) using 2-bromoisobutyryl bromide (BIBB) units as the macroinitiator.[28] ATRP has emerged as a robust tool for the preparation of polymers with well-defined molecular weights, architectures, and chain-end functionalities[29–32] and has been successfully used for the polymerization of a variety of acrylate and methacrylate monomers, such as methyl acrylate,[33,34] *n*-butyl acrylate,[35,36] and methyl methacrylate[37] and the functional monomer 2-hydroxyethyl acrylate[38,39] and its methacrylate analogue 2-hydroxyethyl methacrylate (HEMA).[40] Therefore, by ATRP, a copolymer with excellent properties was obtained, and a microphase-separated system with the hydrophobic domains of the P(BN/NB) main chains and the hydrophilic PHEMA side chains was also formed; this favored proton conductivity. The membranes were further crosslinked with IDA by the esterification of the —OH groups of PHEMA and the —COOH groups of IDA[41,42] and then doped with H_3PO_4 to form imidazole–H_3PO_4 complexes. The generated crosslinks in the membrane offered important benefits, including reduced methanol crossover, good mechanical properties, and excellent thermal stability. The effects of structural variations on the properties of the crosslinked grafted copolymer membranes were studied, and the methanol permeability and the proton conductivity of the new membranes were also given special attention.

EXPERIMENTAL

Materials

5-Norbornene–2-methanol (86.4% endo, 13.7% exo) Chongqing Hi-Tech Chemical Co., Ltd., 98%, (Chongqing, China) was used as obtained from the manufacturer. The catalyst bis(β-ketonaphthylamino) nickel(II), was synthesized according to the method reported in our previous article.[43] Tris(pentafluorophenyl)borane [$B(C_6F_5)_3$, 95%] was purchased from J & K (Beijing, China). 1,1,4,7,10,10-Hexamethyltriethylenetetramine (HMTETA) was provided by Aldrich (Shanghai, China). Acetic anhydride was used without further purification. HEMA (96%), IDA, and sodium hydride (NaH; 60%) were provided by Aladdin (Shanghai, China). Copper(I) bromide (CuBr) and BIBB (97%) were pursued from Alfa Aesar (Tianjin, China). 1-Methyl-2-pyrrolidinone, sodium (Na), and hydrochloric acid (HCl) were purchased from Sinopharm Chemical Reagent Co., Ltd (Shanghai, China).

Synthesis of norbornene–2-methyl acetate (NA)

A 250-mL, three-necked flask equipped with a gas inlet (for N_2), condenser, and dropping funnel was charged with 6.0 mL (0.05 mol) of 5-norbornene–2-methanol (86.4% endo, 13.7% exo) and 100 mL of pyridine. At 20°C, 4.8 mL (0.05 mol) of acetic anhydride was added dropwise over a period of 1 h. The mixture was heated to reflux for 3 h and poured into ice water after it was cooled to room temperature. The crude product was extracted with diethyl ether and washed, first with a 10% aqueous HCl solution and then with an aqueous sodium carbonate solution. The organic fraction was dried over anhydrous sodium sulfate and distilled under reduced pressure.

Yield = 7.7 g (92.8%) of the product. ^{1}H-NMR ($CDCl_3$, δ): 6.07 (m, 2H), 4.13 (d, 1H), 3.94 (d, 1H), 2.82 (m, 1H), 2.68 (m, 1H), 2.05 (s, 3H), 1.69 (m, 1H), 1.31 (m, 2H), 1.27 (m, 1H), 1.13 (d, 1H).

Synthesis of 2-butoxymethylene norbornene (BN)

A 250-mL glass reactor was loaded with 4.8 g (0.2 mol) of NaH and 100 mL of tetrahydrofuran (THF), and then, 6 mL (0.05 mol) of 5-norbornene–2-methanol (86.4% endo, 13.7% exo) was added under stirring at room temperature and refluxed for 2 h. Then, 11 mL (0.1 mol) of bromobutane was added dropwise. We continued to stir the reaction mixture for 24 h at room temperature. After the mixture was washed with deionized water, the organic layer was separated and dried with magnesium sulfate and concentrated by rotary evaporation. The product was purified by column chromatography [SiO_2 with an eluent of petroleum ether–ethyl acetate (4/1 v/v)] and distilled at reduced pressure.

Yield = 7.83 g (87%). ^{1}H-NMR ($CDCl_3$, δ): 6.15–5.90 (m, 2H, CH═CH), 3.8–3.2 (m, 4H, ─CH_2─O─CH_2─), 3.06–0.82 (m, 7H, norbornene–7H), 1.11 (t, 3H, ─CH_3).

All of the monomers were dried over CaH_2 and vacuum-distilled before polymerization.

Synthesis of poly(butoxymethylene norbornene-co-norbornene methyl acetate) [P(BN/NA)]

The copolymerization of BN and NA (molar ratio = 9 : 1) was carried out in a 100-mL, two-necked, round-bottom flask with a magnetic stirring bar and sufficiently purged with nitrogen with a homogeneous bis(β-ketonaphthylamino) nickel(II) catalyst and with $B(C_6F_5)_3$ as a cocatalyst. The appropriate $B(C_6F_5)_3$ solid, anhydrous toluene, 5-NB–2-MeOBu, and 5-NB–2-MeOCOMe were added sequentially to the reactor, and the copolymerization was conducted at 60°C for 6 h. We terminated the polymerization by venting off excess catalyst and adding 5% HCl/EtOH (v/v). The resulting copolymer {weight-average molecular weight (M_w) = 1.2×10^5 g/mol, molecular weight distribution [MWD; M_w/number-average molecular weight (M_n)] = 2.21} was separated off, washed with fresh methanol, and dried *in vacuo* at 40°C until the weight remained constant. The total volume of the liquid phase was kept to 10 mL.

Synthesis of poly(butoxymethylene norbornene-co-norbornene methanol) [P(BN/NOH)]

The counted P(BN/NA) was dissolved in 40 mL of THF/EtOH (5/1 in v/v); then, 10 mL of an NaOH (5 mol/L) solution was added to the refluxing solution dropwise over a period of 1 h and was then refluxed for 24 h. The organic layer was separated and precipitated into 5% HCl/MeOH (v/v). The resulting polymer, PBN/NOH [$M_w = 1.0 \times 10^5$ g/mol, MWD (M_w/M_n) = 1.85], was separated off, washed with fresh methanol and deionized water, and then dried *in vacuo* at 40°C until the weight remained constant. The P(BN/NA) and the P(BN/NOH) were dissolved well in common organic solvents, such as THF, chloroform ($CHCl_3$), toluene, chlorobenzene, and cyclohexane.

Synthesis of P(BN/NB)

After N_2 purging for 30 min, the reaction vessel was immersed in an ice water bath. P(BN/NOH) (0.6 g) was dissolved in 100 mL of THF in a round flask. After a homogeneous polymer solution was obtained, 0.4 mL of BIBB and 0.05 mL of pyridine were successively added, and the reaction flask was sealed with a rubber septum. The reaction was allowed to proceed for 24 h. After the reaction, the product solution was precipitated into methanol. The polymer was purified by redissolution in THF and reprecipitation in methanol and washed with fresh methanol and deionized water. Finally, P(BN/NB) [$M_w = 1.2 \times 10^5$ g/mol, MWD (M_w/M_n) = 2.18] was dried in a vacuum oven overnight 40°C until the weight remained constant at room temperature.

Synthesis of P(BN/NB)-g-PHEMA graft copolymer

After N_2 purging for 30 min, the reaction vessel was immersed in an oil bath at 25°C. P(BN/NB) (0.3 g) was dissolved in 10 mL of THF in a round flask. After a homogeneous polymer solution was obtained, 0.2 mL of HEMA, 0.014 g of CuBr, and 0.05 mL of HMTETA were successively added, and the reaction flask was sealed with a rubber septum. The reaction was allowed to proceed for 6 h. After polymerization, the resulting polymer solution was diluted with THF. After the solution was passed through a column with activated Al_2O_3 to remove the catalyst, the polymer solution was precipitated into methanol. The polymer was purified by redissolution in THF and reprecipitation in methanol. Finally, P(BN/NB)-*g*-PHEMA [$M_w = 1.5 \times 10^5$ g/mol, MWD (M_w/M_n) = 2.29] was dried in a vacuum oven overnight at room temperature.

Preparation of the P(BN/NB)-g-PHEMA/IDA/H3PO4 membranes

The P(BN/NB)-*g*-PHEMA graft copolymer (0.16 g) was dissolved in THF at 8 wt %. Various amounts of IDA and H_3PO_4 were added to the P(BN/NB)-*g*-PHEMA solutions, as shown in Table I. Each polymer solution was cast into a Petri dish after enough ultrasonic dispersion and then dried in an oven at room temperature for 24 h and 80°C for 3 h. Finally, the membranes were crosslinked at 120°C for 3 h.[24]

TABLE I
Concentrations of PHEMA, IDA, and H_3PO_4 in the P(BN/NB)-*g*-PHEMA/IDA/H_3PO_4 Membranes

	Added [PHEMA] : [IDA] : [H_3PO_4] molar ratio
P(BN/NB)-*g*-PHEMA	3 : 0 : 0
P(BN/NB)-*g*-PHEMA311	3 : 1 : 1
P(BN/NB)-*g*-PHEMA322	3 : 2 : 2
P(BN/NB)-*g*-PHEMA333	3 : 3 : 3
P(BN/NB)-*g*-PHEMA344	3 : 4 : 4

Water uptake and dimensional change

The membrane was dried at 80°C *in vacuo* overnight until a constant weight as dry material was obtained. It was immersed into deionized water at room temperature for 48 h. Then, the membranes were taken out, wiped with tissue paper, and quickly weighed on a microbalance. The water uptake and dimensional changes of the membranes were calculated with the following equations:

$$\text{Wateruptake}(\%) = (W_s - W_d)/W_d \times 100\% \quad (1)$$

$$\text{Dgr}; T_c(\%) = (T_s - T_d)/T_d \times 100\% \quad (2)$$

$$\text{Dgr}; L_c(\%) = (L_s - L_d)/L_d \times 100\% \quad (3)$$

where W_d and W_s are the weights of the dried and wet membranes, respectively; T_s, T_d, L_s, and L_d are the thicknesses and lengths of the wet and dried membranes, respectively; and ΔT_c and ΔL_c are the changes in the thickness and length of the membranes, respectively. The water uptake and dimensional changes of the samples were estimated from the average value of at least three measurements for each membrane.

Proton conductivity

The proton conductivities of the membranes at different temperatures were evaluated with three-electrode electrochemical impedance spectra. The impedance measurements were carried out on a CHI660C electrochemical workstation CH Instruments (Austin, Texas, USA) coupled with a computer. A polytetrafluoroethylene diffusion cell composed of two symmetrical chambers was divided by a membrane sample. The cells were filled with an electrolyte composed of sulfuric acid (0.5*M*). The two platinum wires used as a working electrode and counter electrode and an Ag/AgCl electrode functionalized as the reference electrode were introduced into the electrolyte solution. The impedance spectra were recorded with the help of ZPlot/ZView software (CH Instruments, Austin, Texas, USA) under an alternating-current perturbation signal of 10 mV over the frequency range 0.1 MHz to 1 Hz. The electrical resistance of the system (without the membrane divided) was measured as R_1, and the electrical resistance of the system (with the membrane divided) was measured as R_2. The electrical resistance of membrane under various temperatures (30–80°C) at 100% humidity was obtained as the dispersion of R_2 and R_1. The proton conductivity of the membrane was calculated with the following equation:

$$\delta = I/(RA) \quad (4)$$

where δ, I, R, and A represent the proton conductivity, thickness of the membrane, resistance of the membrane, and cross-sectional area of the membrane, respectively.

Methanol permeability

An organic glass diffusion cell was used to obtain the methanol permeability of the membranes. The diffusion cell was composed of two chambers divided by a membrane sample. One chamber of the cell was filled with a 1*M* (C_1) methanol solution in deionized water. The other chamber was filled with deionized water. A sample (effective area = 0.385 cm^2) was clamped between the two chambers. Both compartments were stirred by a magnetic follower during the experiment. The concentration of methanol in solution D was estimated with a differential refractometer WellChrom K-2401) (KNAUER, Wissenschaftliche Gerätebau Dr. Ing. Herbert Knauer GmbH (Berlin, Germany). The refractometer was highly sensitive to methanol, which could be measured continuously during the test. The methanol permeability was calculated from the slope (S) of the straight-line plot of the methanol concentration versus time. The measurement temperature was room temperature. The membrane permeability (P) was calculated with the following equation:

$$P = SV_2l/AC_1 \quad (5)$$

where A (cm^2) is the membrane area, l (cm) is the membrane thickness, C_1 is the methanol concentration, and V_2 is the volume of deionized water.

Characterization of membranes

Fourier transform infrared (FTIR) spectrum spectroscopy was measured on a Shimadzu (Tokyo, Japan) IRPrestige-21 FTIR spectrophotometer. The NMR spectra were collected on a Bruker (Rheinstetten, Germany) ARX 600 NMR spectrometer with deuterated $CHCl_3$ as the solvent and with tetramethylsilane ($\delta = 0$) as the internal standard. Transmission electron microscopy (TEM) images were obtained

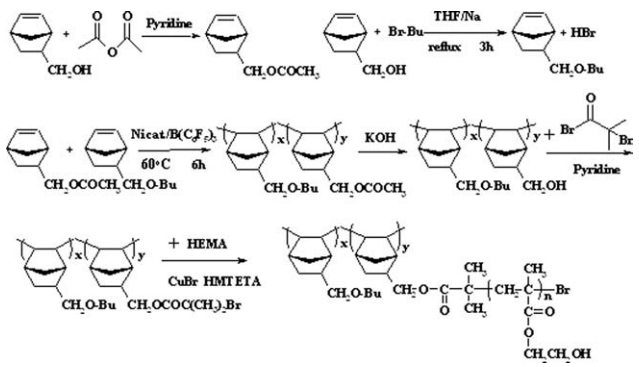

Scheme 1 Illustration of the procedures for the synthesis of P(BN/NB)-*g*-PHEMA.

with a JEOL (Tokyo, Japan) JEM-2010(HR) microscope operated at 200 kV. For the TEM analysis, the polymer sample was dissolved in 1 wt % THF, and samples were prepared by the deposition of a drop of this solution onto standard carbon-coated TEM grids; this allowed the grids to dry without further staining. The wide-angle X-ray diffraction (WAXD) study of the samples was carried out on a Bruker D8 Focus X-ray diffractometer, operating at 40 kV and 40 mA with a copper target (l = 1.54 Å) and at a scanning rate of 2°/min. The tensile strength, elongation at break, and elastic modulus were measured with an CMT8502 machine model GD203A ShenZhen Sans Testing Machine Co., Ltd., China (Shenzhen, China) at a speed of 5 mm/min. Thermogravimetric analysis (TGA) was performed in a nitrogen atmosphere from room temperature to 600°C at a rate of 20°C/min. The degradation of the membranes were measured with the percentage of the weight loss that occurred during the heating process. Gel permeation chromatography (GPC), so-called size-exclusion chromatography analysis, was conducted with a Breeze Waters system equipped with a Rheodyne injector, a 1515 Isocratic pump, and a Waters (Milford, Massachusetts, USA) 2414 differential refractometer with polystyrene as the standard and $CHCl_3$ as the eluent at a flow rate of 1.0 mL/min and 40°C through a Styragel column set, Styragel HT3 and HT4 (19 × 300 mm^2, 10^3 + 10^4Å) to separate the molecular weights, which ranged from 10^2 to 10^6. The instrument was calibrated with monodisperse polystyrene standards.

RESULTS AND DISCUSSION

Synthesis of the P(BN/NB)-g-PHEMA graft copolymer

The reaction scheme for the synthesis of the P(BN/NB)-*g*-PHEMA copolymer via ATRP is illustrated in Scheme 1.[28]

Vinyl-type polynorbornene does not usually dissolve in common organic solvents, such as chlorobenzene, $CHCl_3$, and THF. To increase the solubility of polynorbornene, it is necessary to polymerize functional norbornene monomers.[44] In view of this, we designed the norbornene ester derivative (NA) and norbornene ether derivative (BN) by introducing a flexible alkyl side chain into the rigid norbornene backbone via ester or ether linkages. The copolymerization of NA and BN drastically improved the solubility of the resulting copolymers, especially the copolymer containing 90 mol % BN units, and it readily dissolved in THF, methyl-2-pyrrolidinone, $CHCl_3$, and so on.

As we all know, Ni(II)-based catalysts are of particular interest because they provide polynorbornene (PNB), which has excellent processability.[45] For this reason, the vinyl addition polymerization of the two functional norbornene monomers used homogeneous bis(*b*-ketonaphthylamino) nickel(II) as a catalyst and $B(C_6F_5)_3$ as a cocatalyst. After the de-esterification of the copolymer, bromide functional groups were introduced into the copolymer P(BN/NB) to obtain the macroinitiator of ATRP for the next step via the reaction of P(BN/NOH) with BIBB. Then, Br atoms directly initiated the graft copolymerization of PHEMA from the P(BN/NB) backbones. The graft polymerization was carried out at 25°C for 6 h; the experimental conditions for ATRP were not stringent compared to those in cationic and anionic polymerization.[46] As a result, the amphiphilic comblike copolymer was composed of hydrophobic P(BN/NB) main chains and hydrophilic PHEMA side chains. The successfully synthesized P(BN/NA), P(BN/NOH), P(BN/NB), and P(BN/NB)-*g*-PHEMA copolymers were confirmed by ^{1}H-NMR and FTIR spectroscopy.

In the ^{1}H-NMR spectra (Fig. 1), all of the copolymers exhibited the proton signals of the norbornene skeleton at 0.7–1.7 ppm,[47] norbornene—CH_2—OCH_2— in the BN units at 3.2–3.4 ppm, and norbornene—CH_2—O— in the NA units at 3.7 ppm. Comparing the ^{1}H-NMR spectrum of P(BN/NA) with that of P(BN/NOH), we observed that the peaks at 2.0 ppm, corresponding to —OOC—CH_3, in the spectrum of P(BN/NA) disappeared in that of P(BN/NOH) when the ester groups were converted to hydroxyls. This demonstrated that the de-esterification of P(BN/NA) was complete. In the ^{1}H-NMR spectrum of P(BN/NB)-*g*-PHEMA, the grafting of PHEMA to the copolymer produced peaks in the regions of 4.2, 3.9, and 3.7 ppm associated with the proton signals of PHEMA; this indicated that the PHEMA was successfully grafted by ATRP. The key resonance peaks were assigned to the appropriate protons, as marked in Figure 1. The composition of the graft copolymer was determined from the

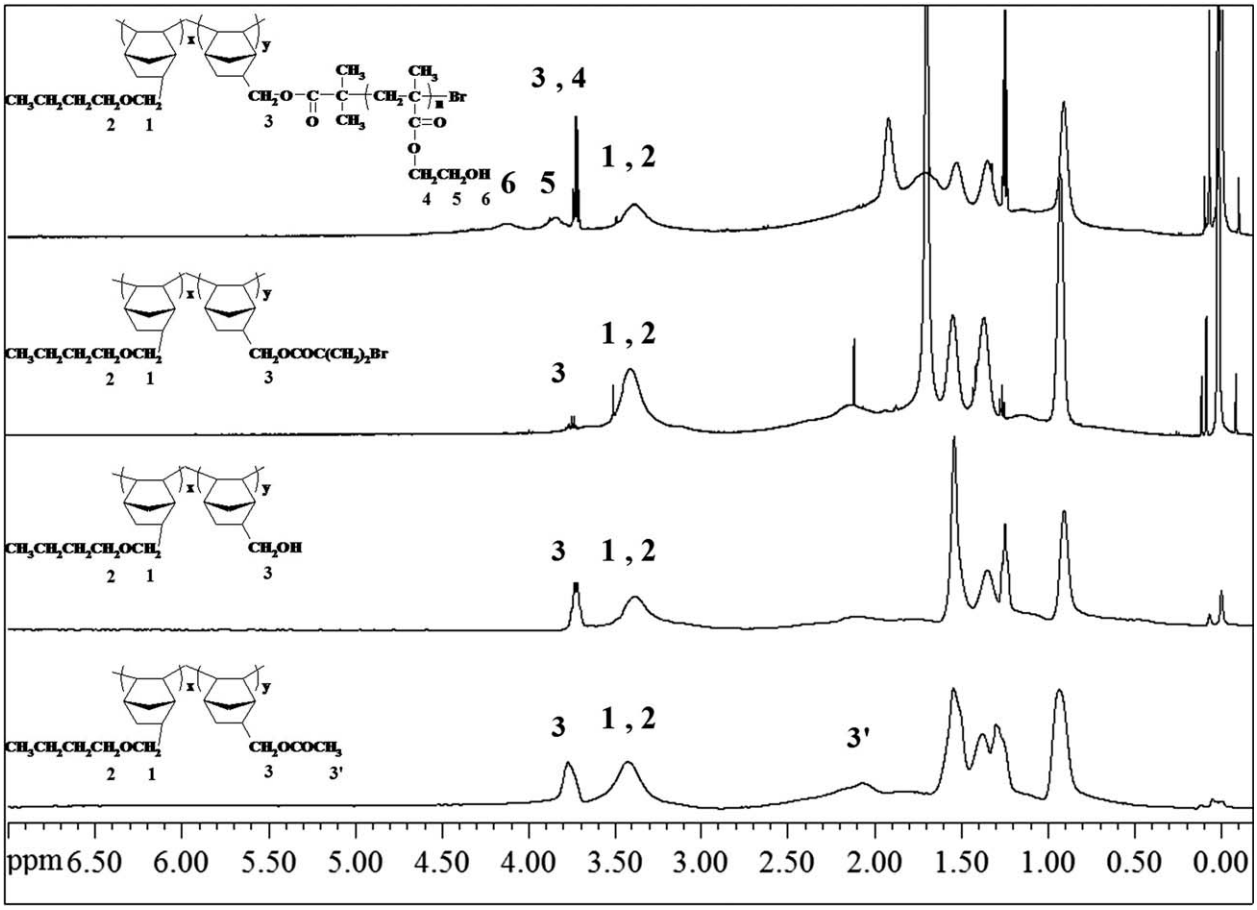

Figure 1 ^{1}H-NMR spectra of the copolymers.

integral ratio of the signals originating from the P(BN/NB) main chains and the PHEMA side chains. As a result, the graft copolymer had a composition of 89 : 11 wt % of P(BN/NB) to PHEMA.

To confirm the chemical structure of the polymers, we collected the FTIR spectra, which are shown in Figure 2. In comparison with that of P(BN/NA), in the spectrum of P(BN/NOH) appeared absorption bands at 3480 cm^{-1} attributed to hydroxyl groups; these indicated that the ester was hydrolyzed and converted successfully to hydroxyl groups. The phenomenon was repeated when P(BN/NB) was grafted with PHEMA, and the copolymer P(BN/NB)-*g*-PHEMA was generated. Thus, the FTIR analyses and ^{1}H-NMR spectra demonstrated that the molecular structure of the grafted copolymer was the expected product.

The morphology of the membranes of polymer architecture plays an important role in their properties, such as proton conductivity, methanol crossover, and water content, and the microphase separation is favorable. TEM analysis was carried out to characterize the morphology of the graft copolymer. Figure 3 presents a TEM image of the synthesized unstained P(BN/NB)-*g*-PHEMA graft copolymer. The difference in the electron densities between P(BN/NB) and PHEMA was sufficiently large enough to provide distinguishable image contrast between the two domains. The micrographs provided direct evidence of biphasic morphology for the polymer membranes. Dark regions represent the hydrophobic domains of the P(BN/NB) main chains, the lighter regions represent the hydrophilic PHEMA side chains, and the big white domains resulted from the evaporated solvents. Hence, the microphase separation structure was obvious.

WAXD is widely used as a powerful tool for investigating the degree of crystallinity of a polymer and the structural changes in proton conducting membranes.[48–51] The WAXD patterns for the P(BN/NB) and P(BN/NB)-*g*-PHEMA grafted copolymer membrane are shown in Figure 4, where the intensity of the X-ray scattering is plotted against the diffraction angle. Two broad halos at 2θ values of 6.7 and 19.1 were observed in both WAXD patterns of the copolymers. The amorphous unsubstituted polynorbornene homopolymer showed two halos at a similar position, and the ester groups substitution decreased the packing density of the polymer.[45] The occurrence of two halos, therefore,

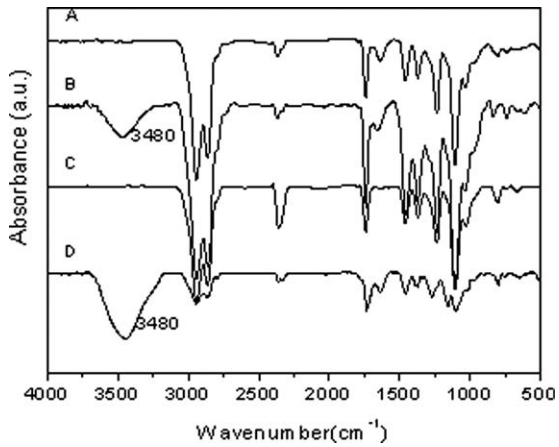

Figure 2 FTIR spectra of copolymers: (A) P(BN/NA), (B) P(BN/NOH), (C) P(BN/NB), and (D) P(BN/NB)-*g*-PHEMA graft copolymer.

revealed that the copolymers were noncrystalline. Compared to P(BN/NB), the intensity of the peak at 19.1° was enhanced in the P(BN/NB)-*g*-PHEMA membrane; this presumably resulted from the grafting of PHEMA from the functional P(BN/NB) backbones.

Preparation of P(BN/NB)-g-PHEMA/IDA/H3PO4

Scheme 2 illustrates the synthesis procedure for the crosslinked P(BN/NB)-*g*-PHEMA/IDA/H_3PO_4 membranes. Through this method, the graft copolymer was crosslinked with IDA via the esterification of the —OH groups of PHEMA and the —COOH groups of IDA, and imidazole–H_3PO_4 complexes were also formed when the membranes were doped with H_3PO_4. The added [PHEMA] : [IDA] : [H_3PO_4] molar ratio of changed from 3 : 0 : 0 to 3 : 4 : 4, as shown in Table I. The doping of one proton from H_3PO_4 onto the imidazole ring of IDA was reasonable, so the molar ratio of IDA to H_3PO_4 was fixed at unity,[24] whereas the molar ratio of the —OH groups of the PHEMA units to the —COOH groups of IDA was varied to investigate the effect of the IDA and H_3PO_4 concentrations.

The FTIR spectra of the P(BN/NB)-*g*-PHEMA and P(BN/NB)-*g*-PHEMA/IDA/H_3PO_4 membranes before and after crosslinking at 120°C for 3 h are presented in Figure 5, and the membrane sample with an added [PHEMA] : [IDA] : [H_3PO_4] molar ratio of 3 : 3 : 3 was used. Compared to the P(BN/NB)-*g*-PHEMA graft copolymer, the P(BN/NB)-*g*-PHEMA/IDA/H_3PO_4 membrane exhibited absorption bands at 3170 cm^{-1}, which were attributable to —NH groups in the membranes.[52,53] The other peaks of —NH groups in the membrane were also shown at 1580 and 1530 cm^{-1}.[27] After it was heated at 120°C for 3 h, the membrane showed slightly stronger absorption bands ascribed to the C—O—C groups from 1250 to 1000 cm^{-1} in the fingerprint region; this demonstrated that the esterification of the —OH groups of PHEMA and the —COOH groups of IDA were carried out, and the membrane was crosslinked successfully. There was no significant spectral change in the membrane before or after thermal treatment, presumably because the concentration of unreacted IDA in the membranes was very low and two or at least one carboxylic acid group of IDA reacted with the —OH group of the graft copolymer.[24]

Proton conductivity and methanol permeability

The proton conductivity and methanol permeability are two transport properties determining the fuel cell performance. A low methanol permeability and good proton conductivity are required for DMFCs.

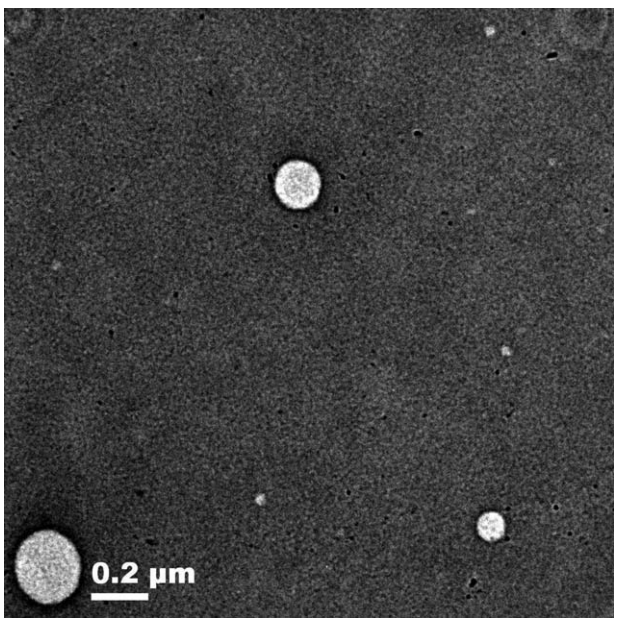

Figure 3 TEM image of the unstained P(BN/NB)-*g*-PHEMA graft copolymer with 11 wt % PHEMA.

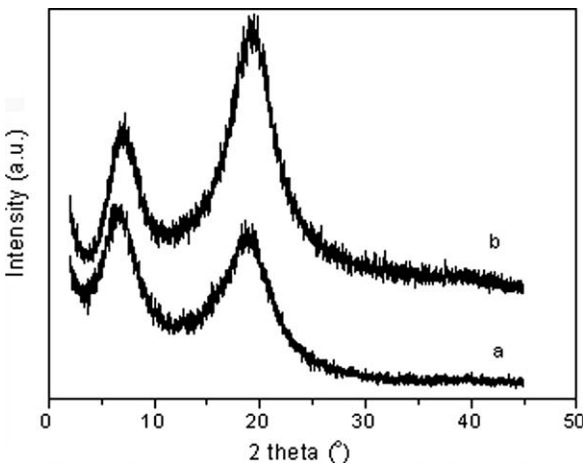

Figure 4 WAXD patterns for pristine (a) P(BN/NB) and (b) P(BN/NB)-*g*-PHEMA graft copolymer with 11% PHEMA.

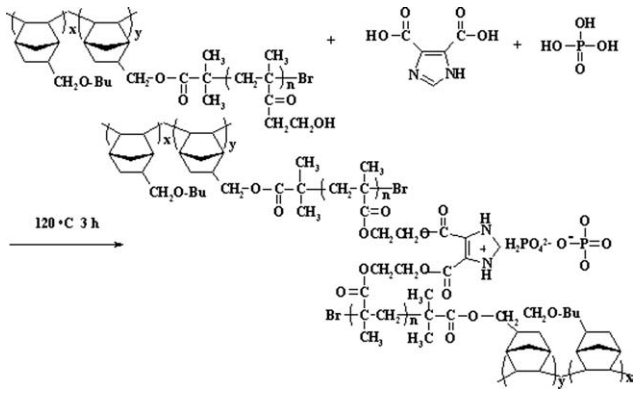

Scheme 2 Procedure for the preparation of the crosslinked membranes.

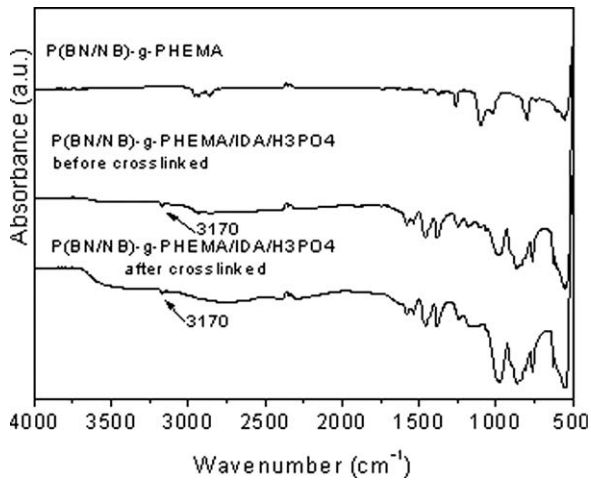

Figure 5 FTIR spectra of P(BN/NB)-*g*-PHEMA and crosslinked membranes before and after crosslinked at 120°C for 3 h.

Proton conductivity can vary with the experimental approach and instruments used.[54] In this study, the proton conductivities were obtained by repeated measurements of the same sample with changing temperature from 30 to 80°C five times and are shown in Table II and Figure 6. The P(BN/NB)-*g*-PHEMA/IDA/H_3PO_4 membrane with [PHEA] : [IDA] : [H_3PO_4] = 3 : 4 : 4 exhibited a maximum conductivity of 0.0043 S/cm at 80°C, at the same order of magnitude to Nafion 115 (0.00793 S/cm). Elevated temperatures favored both the dynamics of proton transport and the structural reorganization of polymeric chains and resulted in an increased proton conductivity.[24] Moreover, with increasing IDA/H_3PO_4 concentration in the membranes, the membrane conductivity also increased because the IDA/H_3PO_4 was the carrier-to-transport proton.

The methanol permeability of the P(BN/NB)-*g*-PHEMA/IDA/H_3PO_4 crosslinked membranes was measured at ambient temperature. The methanol permeability of Nafion 115 was 1.3×10^{-6} cm^2/s. As shown in Table II, the crosslinked vinyl-type polynorbornene structure endowed the membranes with a low methanol permeability. Except for P(BN/NB)-*g*-HEMA344, the methanol permeability of the crosslinked membranes was mostly about one order of magnitude lower than that of Nafion 115. However, the methanol permeability of P(BN/NB)-*g*-HEMA344 slightly increased to 3.8×10^{-6} cm^2/s; this was probably due to some excess IDA and H_3PO_4 uncrosslinked with the PHEMA. The methanol permeability, thus, increased as the IDA and H_3PO_4 content increased. On the basis of these results, we concluded that the incorporation of more IDA/H_3PO_4 improved the proton conductivity and increased the methanol permeability of the membranes as well.

Water uptake and mechanical and thermal properties

Water content is a serious factor and greatly influences the proton transfer of PEMs.[55,56] The water within the membrane provides a carrier for the proton and maintains a high proton conductivity. However, excessive water uptake in a PEM leads to an unacceptable dimensional change or loss of dimensional shape; this can lead to weakness or a dimensional mismatch when the membrane is incorporated into a membrane electrode assembly. The value of water uptake of the membranes were listed in Table II. The water uptake of the crosslinked membranes increased

TABLE II
Properties of the P(BN/NB)-*g*-PHEMA/IDA/H_3PO_4 Membranes

	Water uptake (×100%)	Tensile strength at break (MPa)	Elongation at break (%)	Elastic modulus (MPa)	Proton conductivity at 80°C ($\times 10^{-3}$; S/cm)	Methanol permeability at 20°C ($\times 10^{-6}$; cm^2/s)
P(BN/NB)-*g*-PHEMA	0.8	16.2	3	810.5	—	—
P(BN/NB)-*g*-PHEMA311	44.8	14.4	2.7	692.7	0.08	0.15
P(BN/NB)-*g*-PHEMA322	52.2	13.2	5.2	672.2	0.58	0.20
P(BN/NB)-*g*-PHEMA333	79.2	5.8	26.7	177.3	1.32	0.44
P(BN/NB)-*g*-PHEMA344	123.9	5.5	22.7	159.7	4.30	3.80
Nafion 115	33.4	—	—	110.8	7.93	1.3

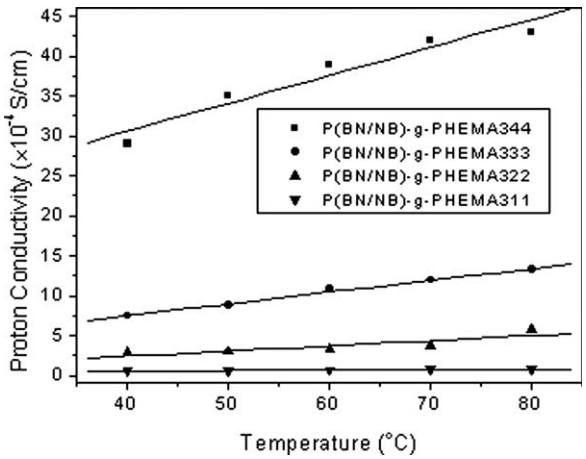

Figure 6 Temperature-dependent proton conductivities of P(BN/NB)-*g*-PHEMA/IDA/H_3PO_4 membranes with different IDA/H_3PO_4 contents.

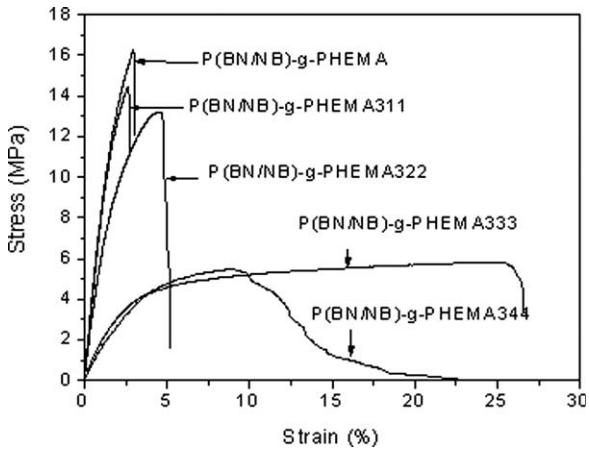

Figure 7 Mechanical properties of P(BN/NB)-*g*-PHEMA/IDA/H_3PO_4 membranes with different IDA/H_3PO_4 contents.

continuously from 0.8 to 123.9 wt % with increasing IDA–H_3PO_4 complex concentrations. This may have been due to the fact that the introduction of H_3PO_4 enhanced the hydrophilicity of the graft polymer membrane and made the membrane store more water. However, there was almost no size change in the crosslinked membrane before and after immersion in deionized water for 10 days; this indicated that the rigid backbone and the crosslinked micromorphology led to a rigid and dense structure in the membrane.

To check the mechanical properties, tensile evaluation was performed on the membranes with Universal testing machine (UTM) at a speed of 5 mm/min, as shown in Figure 7. The tensile strength at break, elongation at break, and elastic modulus for the P(BN/NB)-*g*-PHEMA/IDA/H_3PO_4 membranes with different IDA/H_3PO_4 contents are summarized in Table II. All of the membranes showed good mechanical properties, especially the elastic moduli (from 692.7 to 159.7 MPa), which were much higher than that of Nafion 115 (110.8 MPa). The elongation at break of the membranes (from 2.7 to 22.7%) was enhanced with increasing IDA/H_3PO_4 concentrations; this was due to effective crosslinking in the membranes and the fact that H_3PO_4 made the membranes more flexible. However, the tensile strength (from 14.4 to 5.5 MPa) and elastic modulus did not increase with the crosslinking of the membranes, which did not match with the usual results.[57] Presumably, the imperfect solubility of the IDA/H_3PO_4 in the grafted copolymer solution resulted in the heterogeneous crosslinked structure of the membrane and the destruction of the mechanical properties. However, the crosslinked membranes also exhibited good mechanical properties with normal values of proton conductivity.

Because the application of PEM is often carried out at high temperatures, the thermal stability of the PEM is thus of primary importance. The thermal stabilities of the P(BN/NB)-*g*-PHEMA/IDA/H_3PO_4 membranes were investigated by TGA, as shown in Figure 8. Thanks to the rigid polynorbornene backbone and the crosslinked structure of the

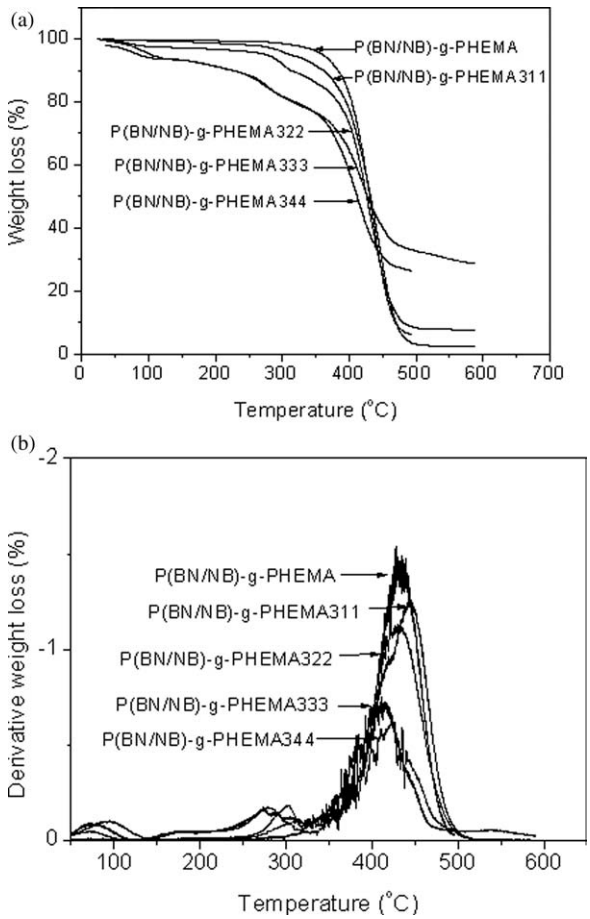

Figure 8 TGA data for P(BN/NB)-*g*-PHEMA/IDA/H_3PO_4 membranes with different IDA/H_3PO_4 contents: (a) weight loss and (b) derivative weight loss.

membranes, the P(BN/NB)-*g*-PHEMA membranes exhibited excellent thermal stability, at least up to 380°C; above this temperature, they started to decompose to around 10 wt %. All of the P(BN/NB)-*g*-PHEMA/IDA/H_3PO_4 crosslinked membranes did not lose weight up to 18 wt % at temperatures as high as above 280°C. The small weight loss of all of the samples below 100°C was mainly due to the loss of water adsorbed in the membrane. The small weight loss of the IDA/H_3PO_4-doped membranes from 280 to 380°C was mainly due to the loss of the crosslinking IDA and the —OH of PHEMA. The residual amounts of membranes increased as the concentration of IDA/H_3PO_4 increased; this indicated that the thermal stability of the PEMs was enhanced by the formation of IDA/H_3PO_4 complexes.[24]

CONCLUSIONS

A new functional vinyl-addition-type polynorbornene graft copolymer membrane, P(BN/NB)-*g*-PHEMA, was prepared by ATRP. A well-defined microphase-separated structure in the comblike copolymer was obtained. After crosslinking with IDA/H_3PO_4, the copolymer proton conducting membranes had a low methanol permeability (from 1.5×10^{-7} to 3.8×10^{-6} cm^2/s). The proton conductivities of the crosslinked membranes were closed to that of Nafion 115 and increased with increasing temperature and content of IDA/H_3PO_4 in the membranes. The tensile strength at break (from 14.4 to 5.5 MPa), elongation at break (from 2.7 to 22.7%), and elastic modulus (from 692.7 to 159.7 MPa) for the P(BN/NB)-*g*-PHEMA/IDA/H_3PO_4 membranes indicated that the PEMs possessed good mechanical properties. In addition, the crosslinked membranes also showed a high thermal decomposition temperature, at least up to 280°C. Thus, this new type of crosslinked membranes could satisfy the requirements of proton-exchange membranes for DMFC applications.

References

1. Bruijn, D. F. Green Chem 2005, 7, 132.
2. Zhu, Y. L.; Liang, J. S.; Liu, C. J Power Sources 2009, 193, 649.
3. Pasupathi, S.; Ji, S.; Bladergroen, B. J.; Linkov, V. J. Hydrogen Energy 2008, 33, 3132.
4. Scott, K.; Shukla, A. K. Rev Environ Sci Biotechnol 2004, 3, 273.
5. Kim, Y. W.; Lee, D. K.; Lee, K. J.; Kim, J. H. Eur Polym J 2008, 44, 932.
6. Xu, H.; Chen, K.; Guo, X. J Membr Sci 2007, 288, 255.
7. Daia, H.; Guan, R.; Li, C. Solid State Ionics 2007, 178, 339.
8. Li, Y.; Wang, F.; Yang, J. J Polym 2006, 47, 4210.
9. Lee, H. S.; Roy, A.; Lane, O. Polymer 2008, 49, 715.
10. Kim, Y. W.; Cho, J. K.; Park, J. T.; Kim, J. H. J Membr Sci 2008, 313, 315.
11. Yeager, H. L.; Steck, A. J Electrochem Soc 1981, 128, 1880.
12. Mauritz, K. A.; Moore, R. B. Chem Rev 2004, 104, 4535.
13. Kreuer, K. D. J Membr Sci 2001, 185, 29.
14. Kreuer, K. D.; Paddison, S. J.; Spohr, E.; Schuster, M Chem Rev 2004, 104, 4637.
15. Qiao, J.; Hamaya, T.; Okada, T. Chem Mater 2005, 17, 2413.
16. Kang, M. S.; Kim, J. H.; Won, J. G. J Membr Sci 2005, 247, 127.
17. Qiao, J.; Hamaya, T.; Okada, T. Polymer 2005, 46, 10809.
18. Hamaya, T.; Inoue, S.; Qiao, J. J Power Sources 2006, 156, 311.
19. Xu, W.; Liu, C.; Xue, X. Solid State Ionics 2004, 171, 121.
20. Rhim, J. W.; Park, H. B.; Lee, C. S. J Membr Sci 2004, 238, 143.
21. Kim, D. S.; Park, H. B.; Rhim, J. W. J Membr Sci 2004, 240, 37.
22. Kim, D. S.; Park, H. B.; Rhim, J. W. Solid State Ionics 2005, 176, 117.
23. Chang, Y. W.; Wang, E. D.; Shin, G. Polym Adv Technol 2007, 18, 535.
24. Kim, Y. W.; Park, J. T.; Koh, J. H.; Roh, D. K.; Kim, J. H. J Membr Sci 2008, 325, 319.
25. Berron, B. J.; Payne, P. A.; Jennings, G. K. Ind Eng Chem Res 2008, 47, 7707.
26. Fei, S. T.; Wood, R. M.; Lee, D. K.; Stone, D. A.; Chang, H. L.; Harry, R. A. J Membr Sci 2008, 320, 206.
27. Vargas, J.; Santiago, A. A.; Tlenkopatchev, M. A. Macromolecules 2007, 40, 563.
28. Zhang, M.; Russell, T. P. Macromolecules 2006, 39, 3531.
29. Matyjaszewski, K.; Xia, J. Chem Rev 2001, 101, 2921.
30. Tsarevsky, N.; Matyjaszewski, K. Chem Rev 2007, 107, 2270.
31. Gao, H.; Matyjaszewski, K. Prog Polym Sci 2009, 34, 317.
32. Matyjaszewski, K.; Tsarevsky, N. V. Nat Chem 2009, 1, 276.
33. Xia, J.; Matyjaszewski, K. Macromolecules 1997, 30, 7697.
34. Davis, K. A.; Paik, H. J.; Matyjaszewski, K. Macromolecules 1999, 32, 1767.
35. Matyjaszewski, K.; Nakagawa, Y.; Jasieczek, C. B. Macromolecules 1998, 31, 1535.
36. Ziegler, M. J.; Matyjaszewski, K. Macromolecules 2001, 34, 415.
37. Wang, J. L.; Grimaud, T.; Matyjaszewski, K. Macromolecules 1997, 30, 6507.
38. Coca, S.; Jasieczek, C. B.; Beers, K. L.; Matyjaszewski, K. J Polym Sci Part A: Polym Chem 1998, 36, 1417.
39. Muhlebach, A.; Gaynor, S. G.; Matyjaszewski, K. Macromolecules 1998, 31, 6046.
40. Yin, M. Z.; Habicher, W. D.; Voit, B. Polymer 2005, 46, 3215.
41. Lee, D. K.; Kim, Y. W.; Choi, J. K.; Min, B. R.; Kim, J. H. J Appl Polym Sci 2008, 107, 819.
42. Kim, D. S.; Park, H. B.; Rhim, J. W.; Lee, Y. M. J Membr Sci 2004, 240, 37.
43. He, X. H.; Yao, Y. Z.; Luo, X. Organometallics 2003, 22, 4952.
44. Oh, S.; Lee, J. K.; Theato, P.; Char, K. Chem Mater 2008, 20, 6974.
45. He, F. P.; Chen, Y. W.; He, X. H.; Chen, M. Q.; Zhou, W. H.; Wu, Q. J Polym Sci Part A: Polym Chem 2009, 47, 3990.
46. Matyjaszewski, K.; Xia, J. Chem Rev 2001, 101, 2921.
47. Tsai, J. C.; Cheng, H. P.; Kuo, J. F.; Huang, Y. H.; Chen, C. Y. J Power Sources 2009, 189, 958.
48. Chuang, S. W.; Hsu, S. L. C.; Hsu, C. L. J Power Sources 2007, 168, 172.
49. Staiti, P.; Lufrano, F.; Aricò, A. S.; Passalacqua, E.; Antonucci, V. J Membr Sci 2001, 188, 71.
50. Staiti, P.; Minutoli, M. J Power Sources 2001, 94, 9.
51. Takamiya, I.; Yamashita, M.; Murotani, E.; Morizawa, Y.; Nozaki, K. J Polym Sci Part A: Polym Chem 2008, 46, 5133.
52. Pu, H.; Wang, D. Electrochim Acta 2006, 51, 5612.
53. Pua, H.; Ye, S.; Wan, D. Electrochim Acta 2007, 52, 5879.
54. Shang, X. Y.; Tian, S. H.; Kong, L. H.; Meng, Y. Z. J Membr Sci 2005, 266, 94.
55. Falcao, S.; Rangel, C. M.; Pinho, C.; Pinto, A. M. F. R. Energy Fuels 2009, 23, 397.
56. Moilanen, D. E.; Spry, D. B.; Fayer, M. D. Langmuir 2008, 24, 3690.
57. Yuan, Y.; Yu, J. J.; Wang, S. S.; Yu, H.; Guan, R. Sci Technol Chem Ind 2009, 172, 166.